Applied Radiation and Isotopes xxx (xxxx) xxx–xxx

Contents lists available at ScienceDirect

Applied Radiation and Isotopes

journal homepage: www.elsevier.com/locate/apradiso

Feasibility of dose enhancement assessment: Preliminary results by means of Gd-infused polymer gel dosimeter and Monte Carlo study

M. Santibáñez[a,b,*], Y. Guillen[a], D. Chacón[c,d], R.G. Figueroa[a,b], M. Valente[a,b,c,e]

[a] Departamento de Ciencias Físicas, Universidad de La Frontera, F. Salazar, 01145 Temuco, Chile
[b] Centro de Física e Ingeniería en Medicina - CFIM, Universidad de La Frontera, Temuco, Chile
[c] Laboratorio de Investigación e Instrumentación en Física Aplicada a la Medicina e Imágenes por Rayos X (LIIFAMIRx), Universidad Nacional de Córdoba, Av. M. Allende s/n, Argentina
[d] Departamento de Física, Universidad Nacional, Heredia, Costa Rica
[e] Instituto de Física E. Gaviola – CONICET, Argentina

HIGHLIGHTS

- Novel Gd-infused PAGAT polymer gel dosimeters for evaluation of absolute dose enhancement.
- Irradiation with ^{241}Am sources combined with Gd doped inside tumor, like alternative brachytherapy source of high dose enhancement.
- Monte Carlo determination of Dose-enhancement by non-symmetrical narrow incident spectrum, centered near to the absorption edge.

ARTICLE INFO

Keywords:
Gd dose enhancement
PAGAT gel dosimetry
Electronic Brachytherapy

ABSTRACT

This work reports the experimental development of an integral Gd-infused dosimeter suitable for Gd dose enhancement assessment along with Monte Carlo simulations applied to determine the dose enhancement by radioactive and X-ray sources of interest in conventional and electronic brachytherapy. In this context, capability to elaborate a stable and reliable Gd-infused dosimeter was the first goal aimed at direct and accurate measurements of dose enhancement due to Gd presence. Dose-response was characterized for standard and Gd-infused PAGAT polymer gel dosimeters by means of optical transmission/absorbance. The developed Gd-infused PAGAT dosimeters demonstrated to be stable presenting similar dose-response as standard PAGAT within a linear trend up to 13 Gy along with good post-irradiation readout stability verified at 24 and 48 h. Additionally, dose enhancement was evaluated for Gd-infused PAGAT dosimeters by means of Monte Carlo (PENELOPE) simulations considering scenarios for isotopic and X-ray generator sources. The obtained results demonstrated the feasibility of obtaining a maximum enhancement around of (14 ± 1)% for ^{192}Ir source and an average enhancement of (70 ± 13)% for ^{241}Am. However, dose enhancement up to (267 ± 18)% may be achieved if suitable filtering is added to the ^{241}Am source. On the other hand, optimized X-ray spectra may attain dose enhancements up to (253 ± 22) %, which constitutes a promising future alternative for replacing radioactive sources by implementing electronic brachytherapy achieving high dose levels.

1. Introduction

Nowadays, infusion of high atomic number elements within biological tissue represents one of the most promising technologies aimed at imaging and therapeutic medical tasks, like tumor targeting, real-time monitoring and dose enhancement (Hainfeld et al., 2004; Ngwa et al., 2014). It is well known that Gadolinium has proven to be an excellent contrast agent for traditional absorption contrast medical imaging (Fujimoto et al., 2009). However, Gd is being considered for different medical tasks regarding dose enhancement, as preliminary reported for brain tumors treatment (Zhang et al., 2014; Prezado et al., 2009).

Different works have addressed the determination of dose enhancement by Gd in different geometries and materials by Monte Carlo simulation. Traditional sources used in brachytherapy, such as: ^{192}Ir, ^{137}Cs and ^{60}Co, have been reported by (Banoqitah and Djouider, 2016; Delorme et al., 2017; Zhang et al., 2014), finding a dependence of the dose enhancement with the Gd concentration in the tumor region, and the inverse dependence with excitation energy, for energy higher than

* Corresponding author at: Centro de Física e Ingeniería en Medicina - CFIM, Universidad de La Frontera, Temuco, Chile.
E-mail address: mauricio.santibanez@ufrontera.cl (M. Santibáñez).

https://doi.org/10.1016/j.apradiso.2018.04.016
Received 15 December 2017; Received in revised form 22 March 2018; Accepted 5 April 2018

the absorption edge of Gd (50.6 keV) given the dependence of $1/E^3$ of the photoelectric absorption. Simulations performed considering concentrations of 20–70 mg/ml have shown maximum dose enhancement of 15% (Zhang et al., 2014) to 45% (Banoqitah and Djouider, 2016) for the case of irradiation with ^{192}Ir, of 8–22% for irradiation with ^{137}Cs (Banoqitah and Djouider, 2016) and from 6% to 15% with ^{60}Co (Banoqitah and Djouider, 2016; Djouider, 2016). Delorme et al. and Prezado et al. have studied the enhancement dose achieved through monochromatic beams, performing energy scanning with beam of energy ranging of 51–200 keV that be able produced by synchrotron facilities, showing the existence of dose enhancement for energies above the absorption edge with maximums in the range of 58–65 keV, with a marked decrease for major energies. In this same line, the work of Delorme et al. reports the comparison between the dose enhancement achieved by Gd nanoparticles with respect to the use of Gd compounds used in NMR, showing comparable results of dose enhancement for both modalities of Gd agents, evidencing only differences in the energy with produce the maximum dose enhancement, possibly due to the effect that the coating of the nanoparticle can play.

The experimental measurement of the absolute dose enhancement involves strong difficulties mainly due to the requirement of achieving an almost uniform distribution of the high atomic number element within the radio-sensitive dosimetric material. Relative dosimetry measurements have been performed by means of different mechanisms mainly based on radiochromic films EBT2 and EBT3 (Ahmad et al., 2016; Cho et al., 2016). The reported results highlight that high levels of sensitivity are actually necessary in order to allow discrimination of low levels of dose enhancement, given that the contribution of Auger electrons and photo-electrons may not be able to reach the radio-sensitive substrate of the radiochromic films, due to the thickness (around to the 100 μm) that separates the radio-sensitive substrate from the solution containing the element of high Z, and only the characteristic X-ray photons will deposit the energy in these dosimeters.

The polymer gel dosimeters are known to able to register and quantify the absorbed dose because of the formation of hydrogels (Baldock et al., 2010). One of the main advantages of polymer over other types of gel dosimeters regards the preservation of the information over time after the irradiation. Formation of hydrogel and/or polymer chains produces density changes clearly correlated to the ionizing radiation exposure of the sensitive material, reading by optical transmission methods (Wuu and Xu, 2011).

PAGAT (PAG And THPC) is a type of polymer gel based in N,N′-methylene-bis-acrylamide (bis) and Acrylamide (AA), combined with the anti-oxidant Tetrakis (hydroxymethyl), Phosphonium Chloride (THPC), which have been widely studied (Venning et al., 2005; Vedelago et al., 2016). The effects of infusing PAGAT polymer gel dosimeters with gadolinium aimed at obtaining an integral stable dosimetry system capable of suitable separation of the different dosimetry components/contributions in order to assess therapeutic dose enhancement due to the selective uptake of high atomic number elements -such as Gd- in biological tissues still remains as a poorly explored research area. In this context, capability to elaborate stable and still dosimetry reactive solution is the first step to accomplish the proposed goal of achieving reliable and accurate measurements of dose enhancement due to Gd presence.

The interest of being able to use this dose enhancement in the brachytherapy techniques, and the existence of energies that would maximize the dose enhancement, motivate the exploration of the benefits of using isotopes with characteristic emissions of energies within the range that maximize the enhancement, such as ^{241}Am (59 keV). As known, the main goal in terms of increasing dose enhancement regards the increase of the photoelectric absorption. It may be expected that irradiating with energies near to the Gd absorption K-edge, like 59 keV Gamma photons (35.7% probability per decay, Almalki et al., 2010) from ^{241}Am sources may produce higher dose enhancements when compared with traditional ^{192}Ir, ^{137}Cs and ^{60}Co brachytherapy sources. Current progress in electronic brachytherapy may suggest the future replacement of radioactive sources by X-ray tubes of 50–75 kV (Dickler, 2009; Garcia-Martinez et al., 2014), hence promoting the study of mini X-ray tubes settings to produce narrow spectra (Santibañez et al., 2016; Santibañez et al., 2017), centered on a specific energy maximizing the photoelectric absorption of Gd K-edge that can be used to increase the dose enhancement, with accessible costs in routine clinical applications, which they would not offer the use of synchrotron beams reports currently.

In this work, a novel dosimetry system was prepared following similar synthesis as for standard PAGAT dosimeter, but including suitable adaptations to add Gd-based solutions (Omniscan®) obtaining a final stable material whose dose-response was carefully characterized. Chemical composition along with exact geometrical and physical properties of the standard and Gd-infused PAGAT dosimeters were introduced to Monte Carlo simulations based on the PENELOPE code in order to evaluate spatial distribution of dose enhancement produced by ^{192}Ir and ^{241}Am. These studies contribute to the evaluation of potential feasibility of replacing the traditional ^{192}Ir source by Am sources (Patent US4510924) in combination with the process of Gd embedded inside the tumor region. Additionally, spatial distribution of dose enhancement was evaluated considering different suitably configured X-ray spectra recently reported for applications aimed at incrementing Gd Kα X-ray fluorescence (Santibañez et al., 2016).

2. Methodology

2.1. Composition of Gd-infused polymer PAGAT dosimeter

The polymer PAGAT dosimeter with the addition of Gadolinium in a final concentration of 20 mg/ml, was manufactured based on the method described elsewhere (Mattea et al., 2013; Vedelago et al., 2016). Gadodiamida solution (Omniscan ®) at 0.5 M was initially diluted in ultrapure deionized water mixing the solution during 20 min at room temperature obtaining a Gd solution with a concentration of 0.26 M. The only variation for Gd-infused PAGAT consisted on replacing water in Mattea et al., 2013; Vedelago et al., 2016 protocol by the previously prepared Gd solution. Gelatin from porcine skin (250 bloom FLUKA) and an H_2O electrolytic solution (90% of the total used) are mixed at room temperature for 10 min into an aluminum-covered flask in order to avoid photo-reaction of the compounds. Subsequently, the temperature is increased to 45 °C in order to achieve homogeneity in the mixture. BIS (N,N`-Methylenbis acrylamide) is added to the previous solution, maintaining the temperature of the mixture for 15 min, being subsequently decreased to 37 °C. Acrylamide (AAM) is added to the mixture maintaining the temperature until its total dissolution, decreasing later until 35 °C. Tetrakis hydrroxymethyl phosphonium choride (THPC) is dissolved in electrolytic H_2O solution (10% of the total used) and added to the previous mixture for 2 min Table 1 summarizes the used chemical composition. Finally, the obtained solution is transferred to dosimeter containers ($4 \times 1 \times 1$ cm^3 spectrophotometry vials), which are kept covered with aluminum to avoid photo-reaction, stored in an oxygen-free environment and refrigerated at 4 °C until 2 h. Fig. 1 shows typical dosimeter samples. Visually, no differences were observed between standard and Gd-infused PAGAT polymer

Table 1
Composition of the Gd-infused polymer PAGAT dosimeter.

Compound	Amount
H_2O electrolitic solution	108.0592 g
Omniscam RMN constrast (287 mg/ml of Gadodiamida)	47.8257 g
Galatin from porcine skin 250 bloom (FLUKA)	8.7579 g
N,N′ Methylenebis acrylamide at 99% (Sigma-Aldrich)	5.251 g
Acrilamide, at 99%	5.2563 g
Tetrakis (hydrroxymethyl) phosphonium choride (THPC) at 80%	300 μl

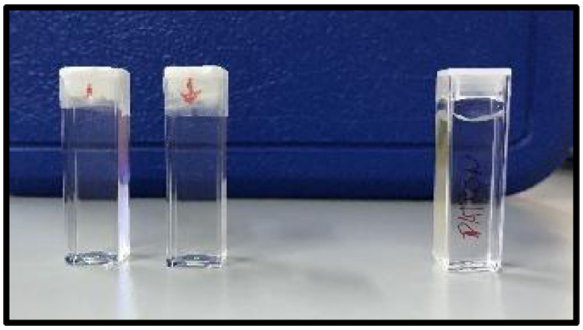

Fig. 1. Gd-infused (left) and standard (right) polymer PAGAT dosimeter samples.

dosimeters.

2.2. Irradiation system for characterization of the dosimeter

The setup used for the irradiation was mounted in the LIIFAMIR^{X} laboratory, which is based on a Kristalloflex X-ray generator (3 kW of maximum power), equipped with a tungsten target and 50 μm Be output window. Dosimeter irradiation was performed setting 44 kVp and 55 kVp with 40 mA and 30 mA tube current, respectively. This configuration allowed to achieve the same dose rate at sample position, which was verified by means of calibrated dosimetry system (PTW 30013 ionization chamber and PTW UNIDOS electrometer), obtaining (200 ± 5) cGy/min at 22 °C of room temperature and (749 ± 3) mmHg pressure. X-ray beam enters the irradiation zone (shielded container), while the sample is located on platform holder perpendicularly to X-ray beam axis. Sample holder rotates continuously aimed at producing more uniform dose distribution inside the sample. Source to sample distance was kept to 41.5 cm representing a field size big enough to cover completely the sample (See Fig. 2).

2.3. Dose-response evaluation and readout stability of Gd-infused PAGAT dosimeters

A set of dosimeters was irradiated by triplicate with doses ranging from 3 to 17 Gy in order to establish the corresponding dose-response for both standard and Gd-infused PAGAT dosimeters by evaluating linearity along with involved uncertainties during measurement process. Irradiation time was fixed according to measured dose rates. The rotating platform served to attain quite uniform dose distribution within dosimeter samples. Before and after irradiation, dosimeter samples were analyzed by a Shimadzu spectrophotometer (UNICO model) evaluating the absorbance differences.

Given that post-irradiation readout is an important characteristic of gel dosimeters, three different batches were prepared for evaluating post-irradiation stability by means of determining absorbance variations, which were evaluated at different times: before irradiation and post-irradiation at 2, 24 and 48 h, scanning always by spectrophotometry within the range 500–600 nm for samples irradiated at dose levels within the same dose range considered for dose-response characterization (3–17 Gy). Except inherent for oxygen contact during sample reading, samples were stored and maintained in identical conditions (no light exposure, 4 °C) between analysis at different post-irradiation times. Finally, samples were irradiated at dose values according to typical linear dose-response of standard (non Gd-infused) polymer gel dosimeters. Because the main goal of the present work consisted on investigating if Gd presence may produce dose enhancement, dose range may not be considered as priority, thus only requiring that irradiations should be performed within linearity range, which did vary significantly when infusing with Gd. according to preliminary studies.

2.4. Monte Carlo simulation

The expected enhancement produced in the novel Gd-infused PAGAT dosimeter by ^{192}Ir, ^{241}Am and X-ray generator were carefully evaluating by means of Monte Carlo simulation. The code used was PENELOPE (version 2008), which is a computational simulation package dedicated to solve electron, photon and positron transport in amorphous materials by means of the Monte Carlo method. It was originally designed to simulate electrons and positrons. The incorporation of photons transport was done later by Sempau et al. (Sempau et al., 1997). The main code is composed of a set of Fortran 77 subroutines that determine physical aspects in the simulation, such as particle interaction, free path, production of secondary particles, etc., by means of transport models and tabulated cross sections data. PENELOPE code has been extensively employed and described in numerous studies involving electron-photon transport as well as it has been thoroughly validated against experimental data (Sempau et al., 2003).

In recent investigations, PENELOPE code has also been used to simulate the effects of using nanoparticles (NPs) on imagenology, pointing out the potentiality for contrast enhancement (Li et al., 2014); and on radiotherapy procedures demonstrating the influence of NPs as radio-sensitizers (Lechtman et al., 2013). All the simulation realized in the work were performed with at least 1×10^9 primary particles ensuring low enough uncertainty (less than 5%) for voxel level dose assessment.

Identical geometry, physical, and chemical properties for dosimeters and radiation source were modeled by Monte Carlo simulation, as shown in Fig. 2b. Mass density of the Gd-infused dosimeter was experimentally determined as 1.048 g/cm^3 corresponding to a concentration of the Gd in the dosimeter of 20 mg/ml. Gd-infused polymer gel materials were defined in PENELOPE by means of *material* subroutine, which enables user to define compounds by means of the additivity rule using the corresponding constituent's fractions by weight. Radiation transport was performed up to cut-off energy (E_{cut}) levels that were fixed to 1 keV for electrons and photons. Once particles reached

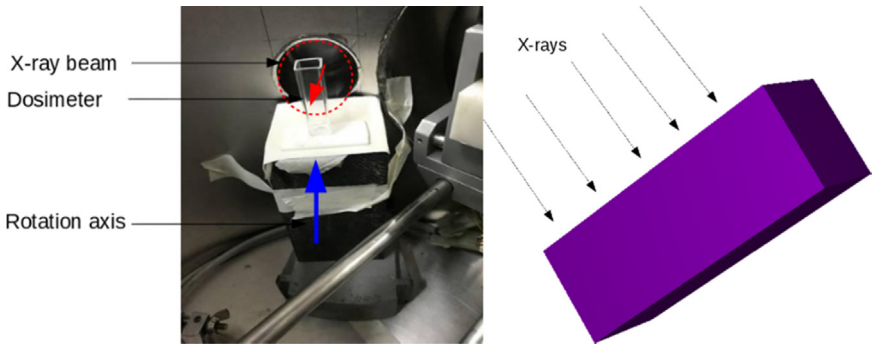

Fig. 2. Irradiation setup picture (left) and sketch based on Monte Carlo geometry (right).

E_{cut} the remaining energy was locally deposited, i.e. in the corresponding tally voxel. Air was included between X-ray source and dosimeter sample. Absorbed dose spatial distribution was calculated using suitable dose tally and defining a regular Cartesian grid defining a 1 mm^3 voxelization. The *penmain* subroutine, part of the PENELOPE package distribution, was adapted for the purposes of the present work and simulations were performed on i7 standard PC, demanding 12 h, approximately for achieving statistical uncertainties lower than 5% in representative cases.

In terms of potential application in brachytherapy, two different sources were used to evaluate the corresponding enhancement: ^{192}Ir (usually employed in brachytherapy) and ^{241}Am given the gamma emission of 59.6 keV, near to the absorption K-edge of the Gd (50.6 keV).

Besides, suitably configured X-ray beams emitting non-symmetrical narrow spectra with FWHM of 9.4 keV (left 5.9 keV and right 3.5 keV), centered at energy slightly above the absorption K-edge (56, 57 and 58 keV) were investigated in accordance with previous works reporting the capability of increasing the spectrum portion able to produce photoelectric absorption (Santibañez et al., 2016).

In a second stage, the effect of the stainless-steel cover (0.15 mm) of the ^{192}Ir in the clinical source was incorporate to correct the incident spectrum produced by this isotope. Additionally, an ad-host cover of 4.3 mm of aluminum was defined to encapsulate the ^{241}Am proportionally reducing the spectral region not capable of K-shell ionization.

The dose enhancement produced by the different sources was evaluated determining the ratio of on-axis depth dose profiles between standard and Gd-infused PAGAT dosimeters. The in-depth dose enhancement was evaluated using 1 mm^2 cross-sectional area and considering different sizes for binning the in-depth axis, obtaining that 1 mm × 1 mm^2 side represented a good balance between relative uncertainties and maintaining small enough volumes.

3. Results and discussions

3.1. Dose-response and stability in the reading of Gd-PAGAT dosimeter

As the first result, it should be stated that the novel Gd-infused polymer PAGAT dosimeters showed no undesired spontaneous reaction and optical properties seem to be not affected when compared with standard PAGAT (see Fig. 1). The Gd-infused PAGAT dosimeter demonstrated good chemical stability with concentration up to 20 mg/ml of Gd (the highest concentration considered in the present work). Fig. 3 shown the visual change in the optical transmittance as a function of the absorbed doses compared with control blank samples without irradiation, for the set of PAGAT and Gd-PAGAT Dosimeters before to be measuring by spectrophotometry.

A linear dose-response is observed for the range of 3–13 Gy (see Fig. 4) after evaluating different intervals of wavelength in the spectrophotometric analysis, similar behavior to previous works (Vedelago et al., 2016). All the intervals of wavelengths allowed to obtain similar degree of linearly in the fitting, with a slightly best value for the interval of 530–540 nm with a R^2 = 0.968 fitting the dose range 3–11 Gy (see Fig. 5).

The stability in the hydrogel formation producing changes in the optical transmission as a function of the ionizing radiation exposure, for the different post-irradiation times shown significant variations, as reported in Fig. 5. The difference between the absorbance reading to 2 h and 24 h of irradiated the dosimeter, for the range of dose studied, was in average a 71 ± 10%, with an 80% for the lowest dose values and 51% for the highest dose. On the other hand, when comparing the difference in the absorbance reading to 24 h and 48 h, it was in average around 3 ± 1%, suggesting that 24 h appears as recommendable option for the readout, which is also in agreement with previous works.

The obtained dose-response in terms of dose levels and system stability constitutes a promising performance for further implementation of Gd-infused PAGAT dosimeters for dose enhancement measurements. As expected, gel dosimeters show low sensitivity for very low dose range, then linear trend is observed, and finally saturation happens for high doses. Therefore, linear fit within the dose range of linear trend may not ensure zero value for the fitting offset.

3.2. Dose-enhancement by ^{192}Ir and ^{241}Am with and without cover

Fig. 6 reports on axis depth dose profiles for standard (red) and 20 mg/ml Gd-infused (blue) PAGAT dosimeters. As expected, increasing tally volume impacts on uncertainty levels. Fig. 6 shows also the percentage dose enhancement produced by (attributable to) gadolinium presence, resulting in an average enhancement of 7 ± 1% with a maximum dose enhancement of 15%.

The Fig. 7 shows the neglected effect in the depth dose when incorporate the cover of the isotope, obtaining similar to configuration of without cover, an average enhancement of 7 ± 1% with a maximum dose enhancement of 13%. These results obtained, show to be concordant to those reported in works (Banoqitah and Djouider, 2016; Zhang et al., 2014) for similar concentrations of Gd, achieving maximum dose enhancements of 12–15% for a concentration of 20 mg/ml.

Dose enhancement due to Americium source in Gd-infused PAGAT dosimeter is reported in Fig. 8. Because ^{241}Am gamma emission is very close to Gd absorption K-edge, higher dose enhancements were achieved when compared with ^{192}Ir source. The average dose enhancement within the sample was estimated as (70 ± 13) %. When evaluating the relative dose enhancement at sample entrance and exit, 98% and 53% were obtained, respectively. Thus, a reduction around 45% was observed for 1.0 cm depth.

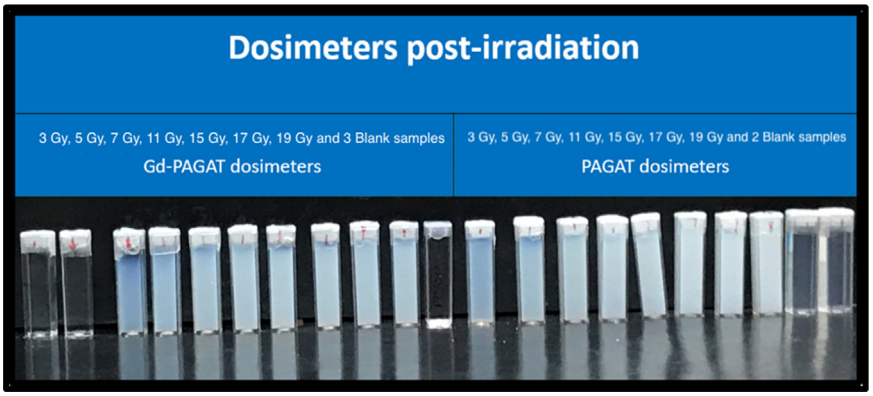

Fig. 3. PAGAT and Gd-PAGAT Dosimeters showing the change in the optical transmittance as a function of the absorbed doses compared with control blank samples without irradiation.

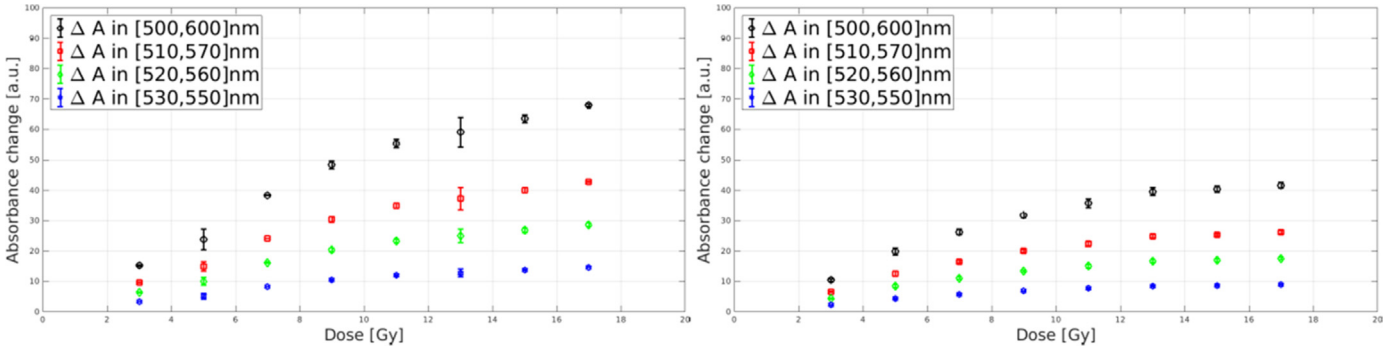

Fig. 4. The absorbance as a function of the dose analyzed at different wavelength intervals for PAGAT (left) and Gd-infused PAGAT (right) dosimeters.

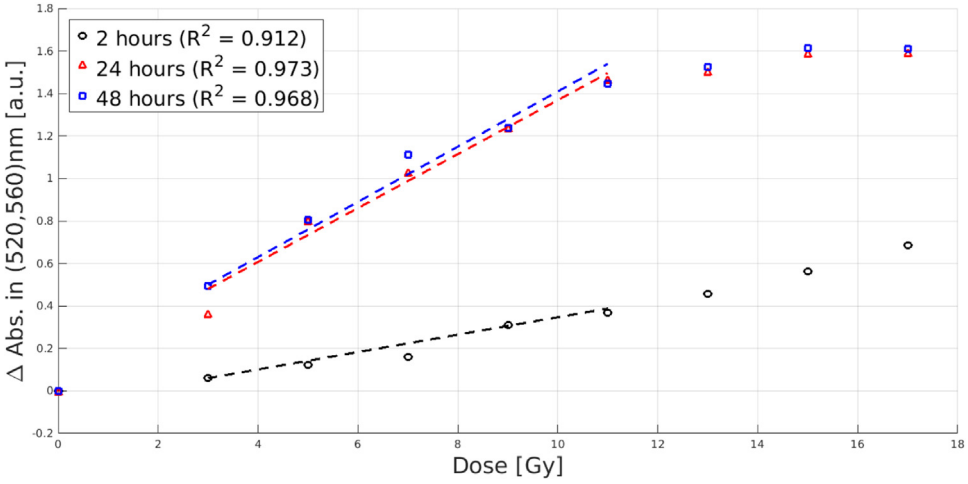

Fig. 5. Absorbance variation within [540, 560] nm for different post-irradiation readout times. Linear regressions performed for [3, 11] Gy. Uncertainties are less than 11%.

The effect of introducing the aluminum cover in the ^{241}Am shown a significant and strong effect in comparison with ^{192}Ir source, producing an average enhancement of (267 ± 18) % (see Fig. 9). Additionally, the enhancement to the entrance and exit of the dosimeter were 293% and 234%, representing a decreasing in the reduction to only 20% for 1.0 cm depth.

Results using ^{241}Am source are not previously reported in the literature, however the strong increase achieved in the dose enhancement

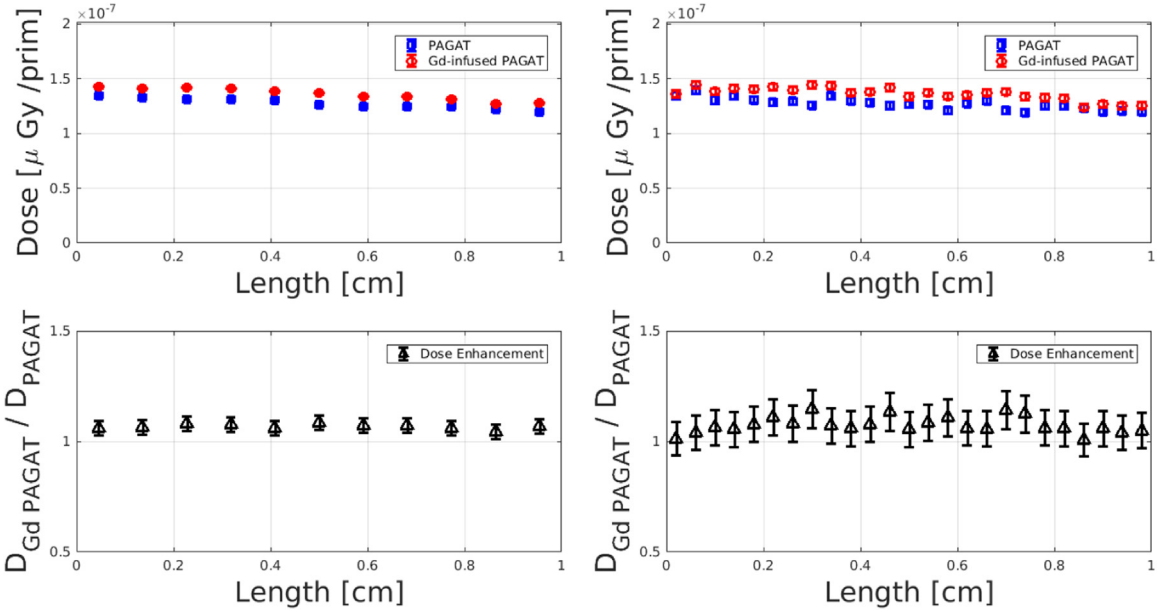

Fig. 6. In-depth dose obtained by Monte Carlo simulations for Gd-PAGAT and PAGAT dosimeters irradiated by ^{192}Ir comparing different sizes of depth binning: 1 mm (left) and 0.4 mm (right).

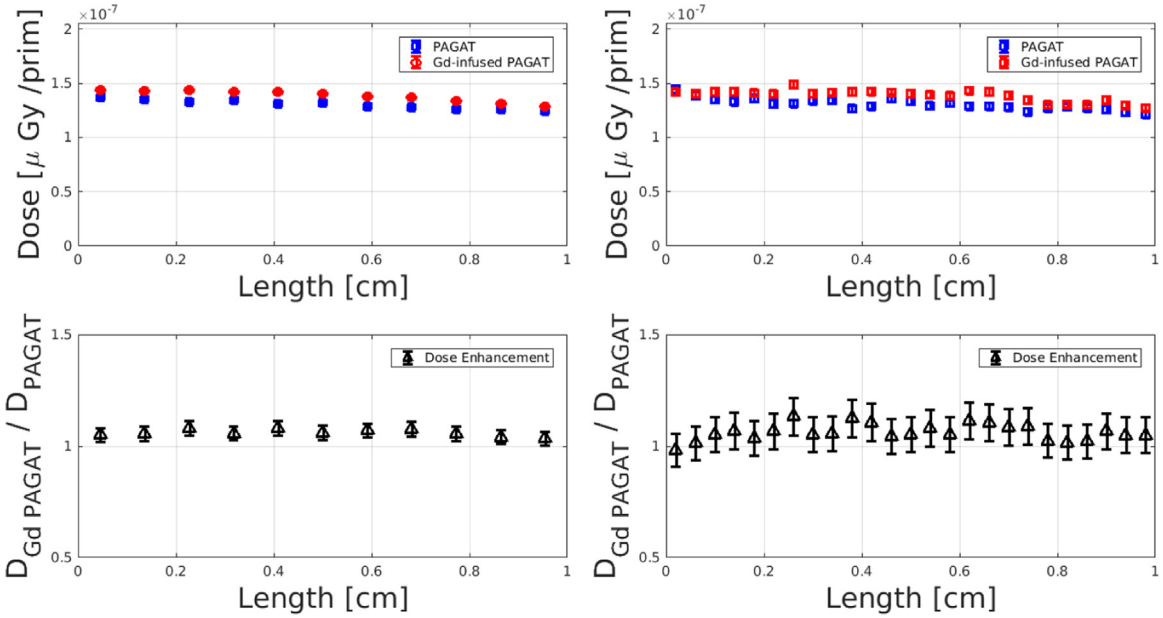

Fig. 7. In-depth dose obtained by Monte Carlo simulations for Gd-PAGAT and PAGAT dosimeters irradiated by ^{192}Ir with stainless steel cover comparing different sizes of depth binning: 1 mm (left) and 0.4 mm (right).

in this work, are in accordance with the predicted with monochromatic beams simulated by (Delorme et al., 2017) for energies of 58 keV with respect to energies between 51 and 200 keV, showing a marked peak in the dose enhancement for energies close to this value.

3.3. Dose-enhancement by optimized X-ray source

Dose enhancement due to X-ray beams emitting non-symmetrical narrow spectra, with a peak central energy among the Gd absorption K-edge as well as 59.6 keV natural gamma emission of ^{241}Am have shown promising performance for potential implementation producing higher dose enhancement (See Fig. 10). Actually, an average percent dose enhancement of (144 ± 10) %, (245 ± 23) %, and (253 ± 22) % were obtained for the spectra centered at 56, 57, and 58 keV, respectively (see Figs. 10–12). Similar to the results were also obtained for ^{241}Am source with cover filter. X-ray beams showed dose enhancement reduction (between entrance and exit dose values) around 21%, 24%, and 23%, respectively (see Figs. 10–12). Likewise, the configuration of X-ray tubes with quasi-monochromatic emission spectra with central energies in the range of 56–58 keV confirm the feasibility of achieving maximum dose enhancement with energies close to 58 keV, showing the same behavior previously achieved with synchrotron beams, but with the feasibility of producing these spectra with the operating energy ranges of the traditional electronic brachytherapy equipment (Dickler, 2009; Garcia-Martinez et al., 2014).

The tuning of an optimized spectrum of X-rays that maximizes dose enhancement, together with the use of high concentrations of Gd, allowed to obtain higher dose enhancement than those reported by other

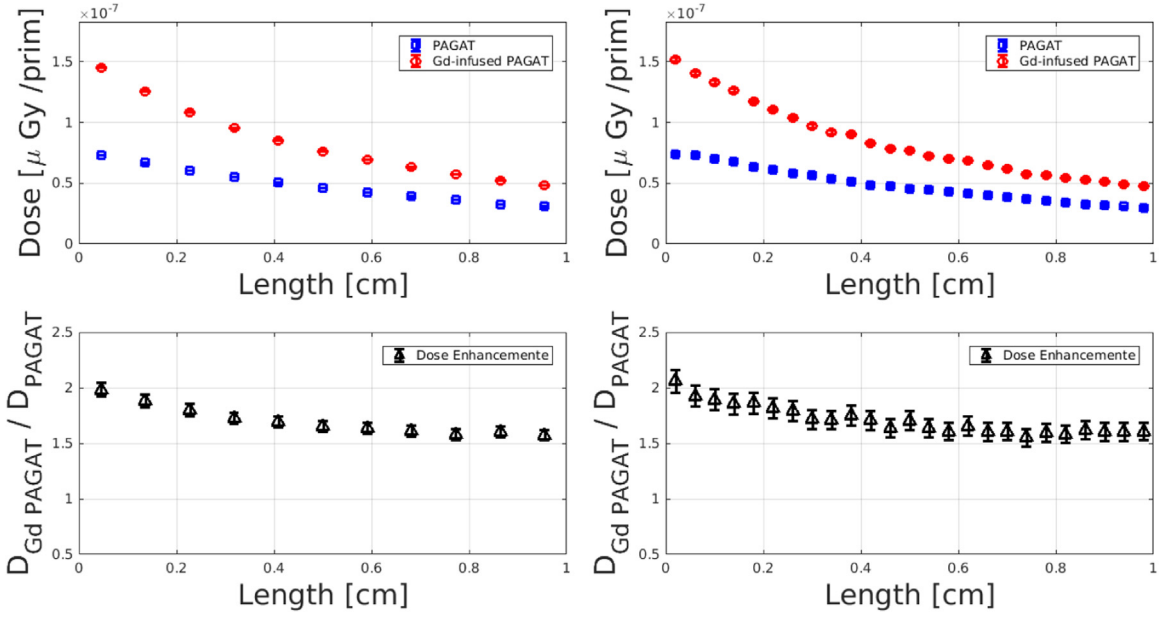

Fig. 8. In-depth dose obtained by Monte Carlo simulations for Gd-PAGAT and PAGAT dosimeters irradiated by ^{241}Am comparing different sizes of depth binning: 1 mm (left) and 0.4 mm (right).

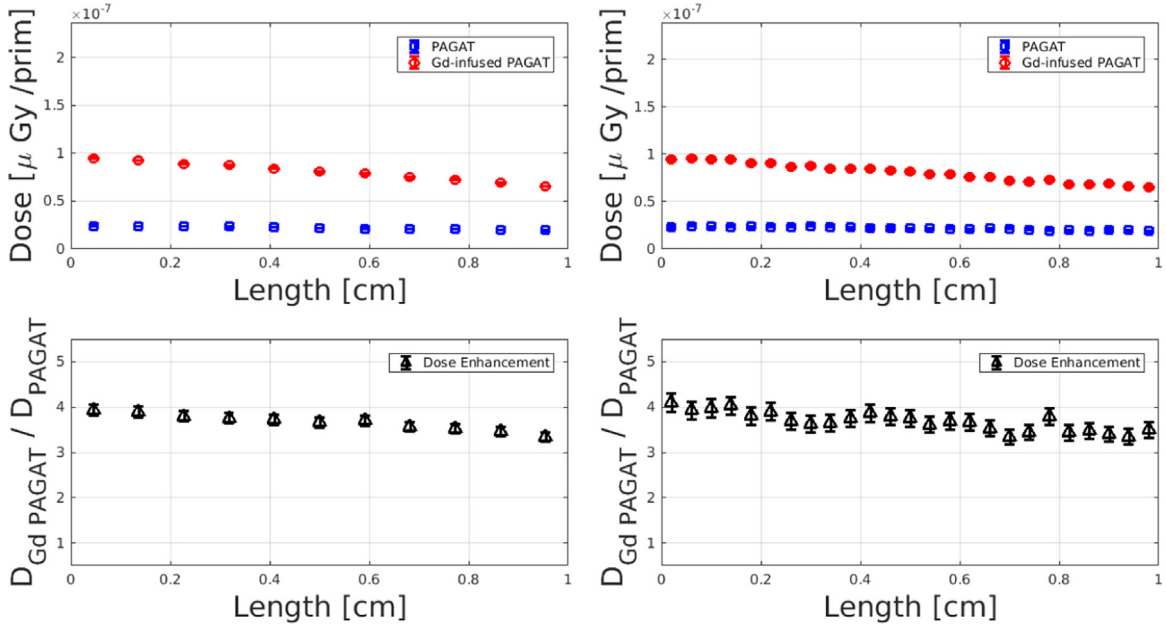

Fig. 9. In-depth dose obtained by Monte Carlo simulations for Gd-PAGAT and PAGAT dosimeters irradiated by ^{241}Am including aluminum cover comparing different sizes of depth binning: 1 mm (left) and 0.4 mm (right).

sources simulated in the literature (reinforcements of 253 ± 22% for the case of spectrum centered on 58 keV and 267 ± 18% for the case of a ^{241}Am spectrum filtering), offer promising results in the feasibility of achieving strong dose increases and be measured experimentally with the generation of the new integral Gd-Pagat dosimeters. Nevertheless, future clinical evaluation requiring to determinate the dose enhancement in anthropomorphic geometry for irradiation by protocol according to the American Brachytherapy Society (Viswanathan et al., 2012) based on the ICRU 38 Report (ICRU, 1985) and the Manchester method. This method defines the measurement (so-called "A") points to be fixed at 2 cm from the central tandem (which contains the guide with the radioactive source) that represent the 100% of dose at tumor target assessed by averaging over a 2 cm radius circle surrounding the tumor target.

4. Conclusions

A novel Gd-infused dosimeter was satisfactory developed, attaining good chemical stability and post-irradiation signal stability. It was further characterized by means of optically analyzed dose-response. Post-irradiation time for sample readout was carefully investigated obtaining that 24 h may be considered for further implementations. The observed linearity dose range appears as very promising for further clinical applications.

Specially adapted subroutines for Monte Carlo simulations confirmed the great potentiality of Monte Carlo techniques to model this type of complex processes. Specifically, it was possible to model a wide variety of radiation sources in terms of their effects on dose enhancement due to interactions with gadolinium distributed within the

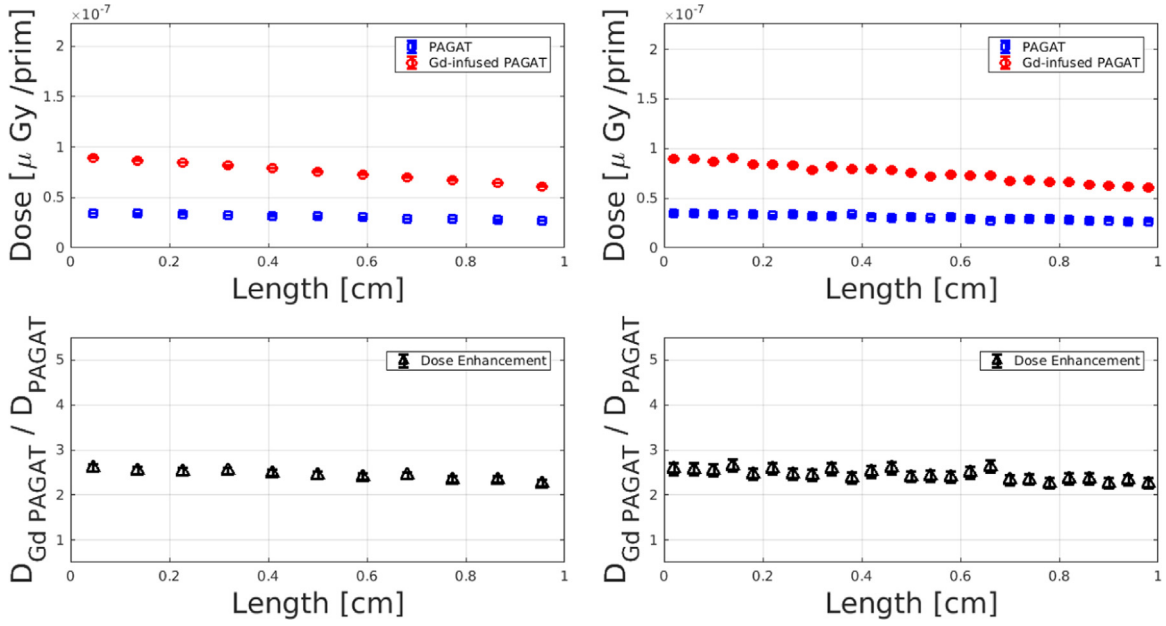

Fig. 10. In-depth dose obtained by Monte Carlo simulations for Gd-PAGAT and PAGAT dosimeters irradiated by non-symmetrical narrow spectrum centered at 56 keV comparing different sizes of depth binning: 1 mm (left) and 0.4 mm (right).

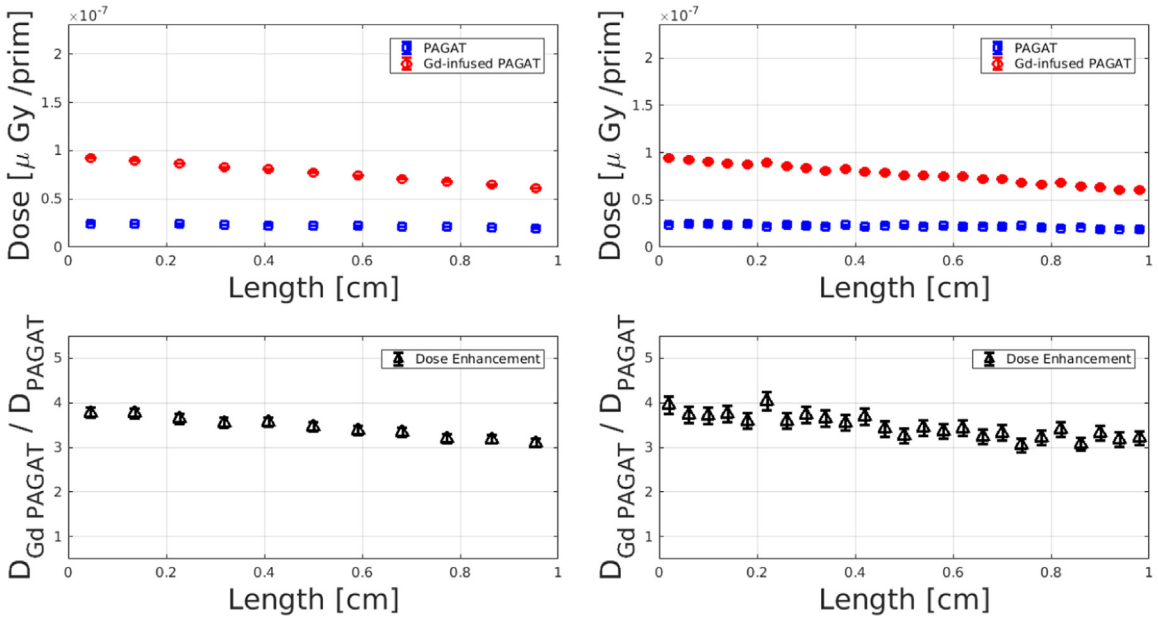

Fig. 11. In-depth dose obtained by Monte Carlo simulations for Gd-PAGAT and PAGAT dosimeters irradiated by non-symmetrical narrow spectrum centered at 57 keV comparing different sizes of depth binning: 1 mm (left) and 0.4 mm (right).

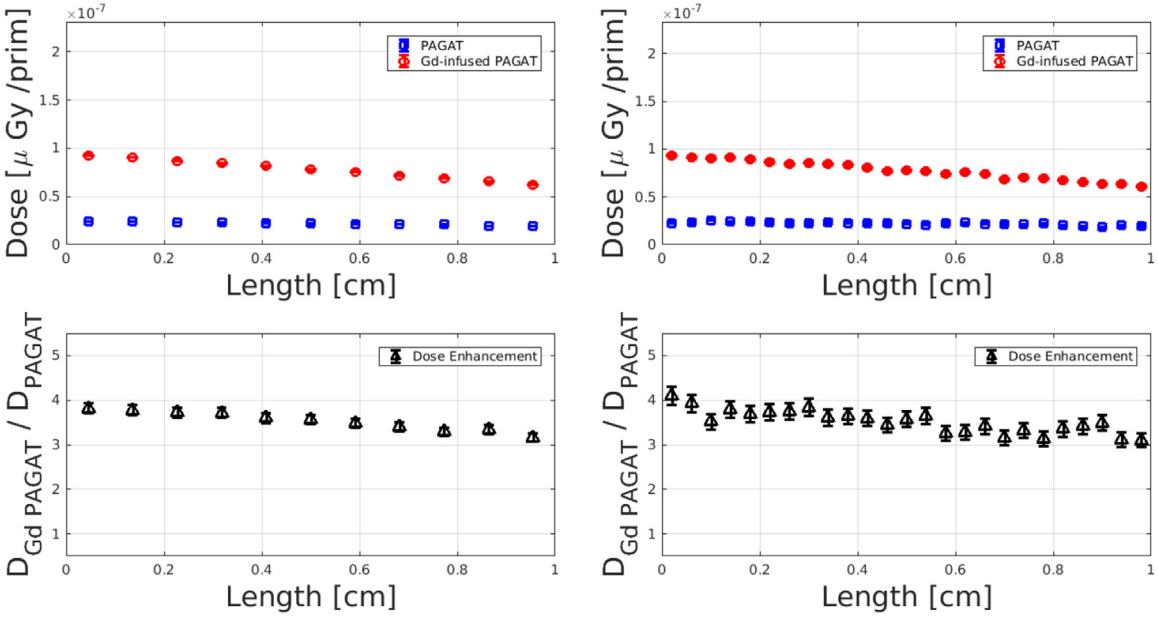

Fig. 12. In-depth dose obtained by Monte Carlo simulations for Gd-PAGAT and PAGAT dosimeters irradiated by non-symmetrical narrow spectrum centered at 58 keV comparing different sizes of depth binning: 1 mm (left) and 0.4 mm (right).

irradiated medium. Moreover, Monte Carlo simulations satisfactorily solved the challenge of attaining spatial distribution of dose enhancement being also capable of assessing reliable quantitative performance of the different studied radiation sources aimed at establishing potentiality, advantages and drawbacks for the different sources. In this context, suitable configured X-ray beams as well as ^{241}Am appear as very promising option when considering potential benefits from gadolinium infusion for dose enhancement purposes.

These results support the feasibility of replacing traditional radioactive isotopes by X-ray source, as already proposed for electronic brachytherapy. This way, configuring X-ray emission spectrum according to Gd properties, it may be suitable to attain significant dosimetry advantages within Gd-doped tumor, like targeting radiotherapy.

Acknowledgements

This work has been supported by the CONICYT program through FONDECYT grant No. 11150673.

References

Ahmad, R., Royle, G., Lourenço, A., Schwarz, M., Fracchiolla, F., Ricketts, K., 2016. Phys. Med. Biol. 61, 4537–4550.
Almalki, M., Majid, S.A., Butler, P.H., Reinisch, L., 2010. Australas. Phys. Eng. Sci. Med. 33, 185–191.
Baldock, C., De Deene, Y., Doran, S., Ibbott, G., Jirasek, A., Lepage, M., McAuley, K., Oldham, M., Schreiner, L., 2010. Phys. Med. Biol. 55, R1eR63.
Banoqitah, E., Djouider, F., 2016. Rad. Phys. Chem. 127, 68–71.
Cho, J., Gonzalez-Lepera, L., Manohar, N., Kerr, M., Krishnan, S., Cho, S.J., 2016. Phys. Med. Biol. 61, 2562–2581.

Delorme, R., taupin, F., flaender, M., ravanat, J.L., champion, Ch., agelou, M., elleaume, H., 2017.
Dickler, A., Dowlatshahi, K., 2009. Expert Rev. Med. Devices 6, 27–31.
Fujimoto, T., Ichikawa, H., Akisue, T., Fujita, I., Kishimoto, K., Hara, H., Imabori, M., Kawamitsu, H., Sharma, P., Brown, S.C., Moudgil, B.M., Fujii, M., Yamamoto, T., Kurosaka, M., Fukumori, Y., 2009. Appl. Radiat. Isot. 67, S355–S358.
Garcia-Martinez, T., Chan, J.P., Perez-Calatayud, J., Ballester, F., 2014. J. Contemp. Brachytherapy 6, 45–53.
Hainfeld, J.F., Slatkin, D.N., Smilowitz, H.M., 2004. Phys. Med. Biol. 49, 309–315.
Lechtman, E., Mashouf, S., Chattopadhyay, N., Keller, B.M., Lai, P., Cai, Z., Reilly, R.M., Pignol, J.-P., 2013. Phys. Med. Biol. 58, 3075–3087.
Li, W.B., Müllner, M., Greiter, M.B., Bissardon, C., Xie, W.Z., Schlatll, H., Oeh, U., Li, J.L., Hoeschen, C., 2014. Proceedings of SPIE 9033, p. 90331K.
Mattea, F., Strumia, M., Valente, M., 2013. Proceedings of X Latin American Symposium on Nuclear Physics and Applications, Uruguay, Vol. PoS (X LASNPA), Proceedings of Science, p. 080.
Ngwa, W., Kumar, R., Sridhar, S., Korideck, H., Zygmanski, P., Cormack, R.A., Berbeco, R., Makrigiorgos, M., 2014. Nanomedicine 9, 1063–1082.
Patent US4510924. Brachitherapy Devices and Methods Employing Americium-241.
Prezado, Y., Fois, G., Le Duc, G., Bravin, A., 2009. Med. Phys. 36, 3568–3574.
Santibáñez, M., Vásquez, M., Figueroa, R.G., Valente, M., 2016. Rad. Phys. Chem. 122, 28–34.
Santibáñez, M., Saavedraa, R., Vásqueza, M., Malano, F., Pérez, P., Valente, M., Figueroa, R.G., 2017. Appl. Radiat. Isot. 129, 19–27.
Sempau, J., Acosta, E., Baro, J., Fernández-Varea, J.M., Salvat, F., 1997. Nucl. Instrum. Methods Phys. Res. B 132, 377–390.
Sempau, J., Fernández-Varea, J.M., Acosta, E., Salvat, F., 2003. Nucl. Instrum. Methods Phys. Res. B 207, 107–123.
Vedelago, J., Chacón Obando, D., Malano, F., Conejeros, R., Figueroa, R., Garcia, D., González, G., Romero, M., Santibáñez, M., Strumia, M., Velásquez, J., Mattea, F., Valente, M., 2016. Rad. Meas. 91, 54–64.
Venning, A.J., Hill, B., Brindha, S., Healy, J., Baldock, C., 2005. Phys. Med. Biol. 50, 3875–3888.
Viswanathan, A.N., Thomadsen, B., 2012. American Brachytherapy Society. Cervical Cancer Recommendations Committee, Brachytherapy, 11, pp. 33–46.
Wuu, C.S., Xu, Y., 2011. Radiat. Meas. 46, 1903e1907.
Zhang, D.G., Feygelman, V., Moros, E.G., Latifi, K., Zhang, G.G., 2014. PLoS One 9, e109389.